ELSEVIER

Applied Surface Science 86 (1995) 457–465

applied surface science

Laser direct writing and instabilities: a one-dimensional approach

N. Arnold *, P.B. Kargl, D. Bauerle

Angewandte Physik, Johannes-Kepler-Universität, A-4040 Linz, Austria

Received 27 May 1994; accepted for publication 20 September 1994

Abstract

Laser direct writing of thermally well-conducting deposits on thermal insulators is described on the basis of a one-dimensional model. Different types of instabilities are discussed. The theoretical results are compared with experimental observations.

1. Introduction

The theoretical analysis of laser direct writing [1] requires the simultaneous solution of several 3D partial differential equations for time-dependent geometries. Such calculations can be performed only numerically on fast computers. While such calculations allow proper simulation of the growth process, they do not provide an understanding of the basic functional dependences observed experimentally.

Subsequently, we will develop a simple 1D model which does not pretend to describe experimental data on direct writing with an accuracy better than 30%–40%. However, this model provides the physical picture of laser direct writing for a wide range of experimental parameters. In particular, it explains the development of oscillations in the width and height of stripes that have been observed within certain parameter intervals.

* Corresponding author. E-mail: nikita.arnold@jk.uni-linz.ac.at; Fax: +43 732 2468 9242.

2. Dimension considerations

Statements based on dimension analysis are valid irrespective of the simplifications made. Let us assume a quasi-stationary temperature distribution, surface absorption, heat transport by conduction only, and a kinetically controlled reaction without changes in latent heat. The problem is then described by the *steady* heat equation for the different materials and the equation of growth. In dimensionless variables these equations include non-linear functions characterising the properties of the materials and depend on only two parameters: $P/K_0T_0w_0$, and v_s/k_0. Here, K_0 is some reference heat conductivity (e.g. of the substrate at T_0), T_0 is the temperature of the surrounding, w_0 the radius of laser focus, k_0 a pre-exponential factor in the growth rate function, P the laser power, and v_s the scanning velocity.

Thus, the *shapes of the structures produced with constant ratios P/w_0 and v_s/k_0 are the same, with the coefficient of proportionality equal to the ratio of w_0 in the experiments* (law of similarity in laser deposition). If this prediction is not confirmed by

experiment, factors that have been ignored play a decisive role.

For high laser powers or small laser focuses, when the characteristic size of the microstructure becomes large in comparison to w_0, the laser can be considered as a point source. Then, the problem possesses only the parameter v_s/k_0 and one combination of parameters with the dimension of a length: $r_0 = P/K_0T_0$. If we normalize to r_0 instead to w_0, P will not enter the equations. Therefore, two deposits are similar, if they were grown with the same ratio v_s/k_0. Linear sizes of microstructures scale proportionally to r_0, and thus to the laser power. Therefore, *qualitative* changes in the shape of deposit should depend only on v_s. Otherwise, the finite size of laser focus is important.

These considerations are valid for arbitrary temperature dependences of heat conductivities, absorption coefficients, and rate function. They permit also *arbitrary* changes in geometry and corresponding absorbances. Dimension considerations have thus a wide range of applicability.

3. General 1D approach

3.1. Main assumptions

In this section we briefly discuss the 1D model presented in Ref. [2]. In addition to the assumptions already made, we consider the deposition of a good heat conductor, for example a metal, on a thermal insulator, i.e. the ratio of heat conductivities $K^* = K_D/K_S \gg 1$ (indexes S and D stand for substrate and deposit, respectively). The heat flux from the region near the laser beam is then directed mainly along the deposited stripe.

3.2. Heat equation

Let the stripe be of uniform shape with height h and width $d = 2r$. The meaning of the main quantities is shown in Fig. 1. Let $\theta = T - T_0$ be the temperature rise, F the cross section of the stripe, and A the absorptivity. $\theta_D(x)$ has the meaning of the temperature rise at the interface deposit–substrate. Because $K^* \gg 1$, θ_D is in first approximation independent of z. For $w_0 \ll r$, the energy balance for a slice of a stripe between x and $x + dx$ can be written as [2]

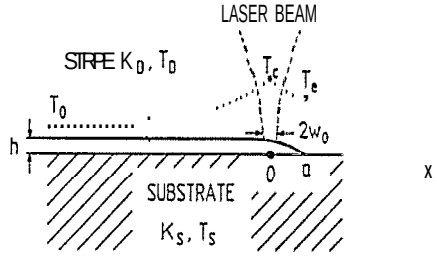

Fig. 1. Schematic picture for laser direct writing. The coordinate system is fixed with the laser beam, The centre of the laser beam of radius w_0 is at the origin $x = 0$; the forward edge of the stripe is at $x = a$. T_c and T_e are the concsponding temperatures. The temperature profile is indicated by the dotted curve. The width of the stripe is $d = 2r$. Temperature at infinity is T_0.

$$l^2 \frac{\partial^2 \theta_D}{\partial x^2} - \theta_D + \frac{PA}{\eta K_S}\delta(x) = 0, \quad \left.\frac{\partial \theta_D}{\partial x}\right|_{x=a} = 0,$$
$$\theta_D|_{x=-\infty} = 0. \qquad (3.1)$$

Here $\eta \approx 2$ characterises losses to the substrate due to heat conduction. $l^2 = FK^*/\eta$ characterises the drop in the laser-induced temperature rise in the x-direction. If the parameters of the stripe are known, the solution of this problem gives the temperature distribution, in particular $\theta_c = \theta_D(x = 0)$ and $\theta_e = \theta_D(x = a)$ [2]. However, these parameters have to be determined self-consistently by taking into account the growth process itself. The cross section and the width of the stripe are characterised by $F = \zeta hr$, $r \approx \xi a$ where ζ and ξ are of the order of unity. With two additional equations provided by assumptions about the temperature at the edge of the stripe and the dynamics of the growth process (see (4.1) or (4.3) and (3.4)) we can determine the unknown quantities.

We consider T_c as a parameter in all important dependences. We then obtain:

$$\mu = \mu(\theta_c) = \operatorname{arccosh}(\theta_c/\theta_e) = \frac{a}{l}, \qquad (3.2a)$$

$$l(\theta_c) = \frac{PA}{\eta K_S \theta_e} e^{-\mu}, \qquad (3.2b)$$

$$r(\theta_c) = \xi a = \xi l \mu = \frac{\xi PA}{\eta K_S \theta_e} \mu\, e^{-\mu}, \qquad (3.3a)$$

$$h(\theta_c) = \frac{\eta}{\zeta K^*}\frac{l^2}{r} = \frac{PA}{\xi\zeta K_D \theta_e}\mu^{-1} e^{-\mu}. \qquad (3.3b)$$

The function μ has been introduced for convenience. From (3.3) we find that K_S influences mainly the width of the stripe, and K_D its height.

3.3. Equation of growth

As in Ref. [2], we write the equation of growth in a coordinate system that is fixed with the laser beam. It is useful to think about the hot area around the laser beam as the 'chemical reactor' [3], where the chemical transformations result in the 'production' of h with the rate $W(T_c)$ given by an Arrhenius-type function with a pre-exponential factor k_0 (cm/s) and activation temperature T_a. This reactor is an open system: The removal of h is provided by the scanning term v, $\partial h/\partial x$ which we approximate by $v_s h/\gamma$a where y ≈ 1. Under stationary conditions this yields

$$v_s(\theta_c) = \gamma a/hW(T_c) = (\gamma\xi\zeta K^*/\eta)\,\mu^2 W(\theta_c + T_0). \quad (3.4)$$

(3.4) and (3.2), (3.3) allow to draw dependences $r(v_s)$, $h(v_s)$, as long as function $\theta_e(\theta_c)$ is known.

4. Conditions at the edge of the stripe

4.1. Systems with temperature threshold

For some systems significant deposition is only observed above certain threshold temperature, T_{th}. An example is the deposition of W from WCl_6 [4]. Then, the temperature at the edge of the stripe is equal to the threshold temperature:

$$\theta_e(\theta_c) = \theta_{th}. \quad (4.1)$$

Corresponding dependences $h(v_s)$, $r(v_s)$, and $T_c(v,)$, are depicted at Fig. 2. The main features of this case are: The widths and heights of stripes are proportional to the laser power. T_c increases with increasing scanning velocity. The height decreases monotonously with v_s. The width shows a non-monotonous dependence on v_s: with small velocities it increases and then starts to decrease. The cross section of the stripe, F a rh, always decreases with v_s.

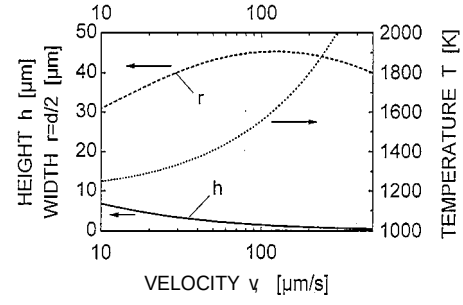

Fig. 2. Typical dependences $h(v_s)$, $r(v_s)$ and $T_c(v_s)$ for systems with threshold behaviour as calculated from (3.2)–(3.4), (4.1) with $\eta = 1.6$, $\zeta = 1.33$, $\xi = 1.25$, $\gamma = 1.3$, $K_D = 8\times10^6$ erg/cm/K, $K_S = 3\times10^5$ erg/cm/K, K * = 26.6, $T_0 = 443$ K, $T_{th} = 1200$ K, $T_a = 2525$ K, $k_0 = 1.6\times10^{-3}$ cm/s, P = 650 mW, $A = 0.55$. Parameters correspond to the deposition of W from WCl_6 on quartz [2].

The characteristics of the stripe in the point of maximum width ($\mu = 1$) are easily calculated from (3.2)–(3.4). The temperature T_c^{max} at which the maximum width is achieved depends only on T_{th}, and v_s^{max} a $W(T_c^{max})$. All of these features are in good agreement with experimental data on the deposition of W lines onto SiO_2 substrates [2,5].

4.2. Systems with high activation energy

If there is no apparent threshold for deposition, the borders of the stripe are determined by the localisation of the chemical reaction, i.e. the deposition rate at the border drops significantly, in comparison to the rate in the hottest region:

$$W(T_e) = e^{-\beta} W(T_c), \quad (4.2)$$

with β about unity (detailed estimations yield $\beta \approx \pi/\gamma^2$). Then, for the Arrhenius rate function:

$$T_e^{-1} = \beta T_a^{-1} + T_c^{-1}, \quad (4.3a)$$

or

$$\theta_e(\theta_c) = \left(\beta T_a^{-1} + (\theta_c + T_0)^{-1}\right)^{-1} - T_0. \quad (4.3b)$$

This expression should now be used instead of (4.1). A typical graph is presented at Fig. 3. It can be shown that μ increases monotonously with θ_c for reasonable values of T_0, T_c, and T_a. Both the height and the width of the stripes, decrease monotonously

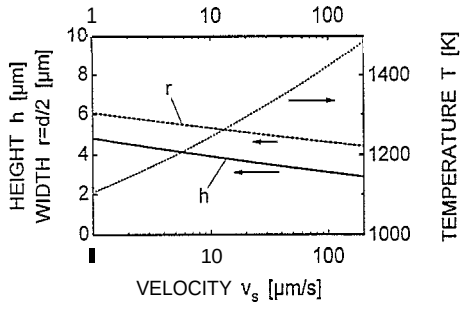

Fig. 3. Typical dependences $h(v_s)$, $r(v_s)$ and $T_c(v_s)$ for systems with high activation energy and no threshold. Calculations have been performed on the basis of (3.2)–(3.4), (4.4) with $\eta = 1.6$, $\zeta = 1.33$, $\xi = 1.0$, $\gamma = 1.3$, $\beta = 1.8$, $K_D = 1.5\times10^6$ erg/cm/K, $K_S = 2.5\times10^5$ erg/cm/K, $K^* = 6$, $T_0 = 300$ K, $T_a = 22000$ K, $k_0 = 2.7\times10^4$ cm/s, P = 100 mW, A = 0.57.

with μ and scanning velocity. If the activation temperature is very high, i.e. $T_a \gg T_c \approx \theta_c \gg T_0$:

$$\theta_e(\theta_c) \approx \theta_c\left(1 - \frac{\beta T_c^2}{T_a\theta_c}\right) \approx \theta_c\left(1 - \frac{\beta\theta_c}{T_a}\right),$$

$$\mu \approx \left(\frac{2\beta T_c^2}{T_a\theta_c}\right)^{1/2} \approx \left(\frac{2\beta\theta_c}{T_a}\right)^{1/2} \ll 1, \qquad (4.4a)$$

$$r(\theta_c) \approx \frac{\xi PA}{\eta K_S}\left(\frac{2\beta}{T_a\theta_c}\right)^{1/2},$$

$$h(\theta_c) \approx \frac{PA}{\xi\zeta K_D}\left(\frac{T_a}{2\beta\theta_c^3}\right)^{1/2}, \qquad (4.4b)$$

$$v_s(\theta_c) \approx \frac{2\beta\gamma\xi\zeta K^*}{\eta}\frac{\theta_c}{T_a}W(T_c). \qquad (4.4c)$$

From (4.4) we obtain the approximate dependences:

$$r(v_s) \approx \frac{(2\beta)^{1/2}\xi}{\eta}\frac{PA}{K_S T_a}\left[\ln\left(\frac{v_0}{v_s}\right)\right]^{1/2},$$

$$h(v_s) \approx \frac{1}{(2\beta)^{1/2}\xi\zeta}\frac{PA}{K_D T_a}\left[\ln\left(\frac{v_0}{v_s}\right)\right]^{3/2},$$

with

$$v_0 = \frac{2\beta\xi\zeta\gamma K^*}{\eta}\frac{\theta_c}{T_a}k_0.$$

Both the height and the width drop off rapidly with v_s. This was in fact observed in many experiments [1,6].

5. Refinements of the general model

We will now study in further detail the influence of the laser focus and temperature-dependent heat conductivities.

5.1. Finite laser focus w_0

With low laser powers, the width of stripes, given by (3.3), can become comparable to w_0. Then, the laser beam cannot be considered as a point source. The temperature distribution cannot become much narrower than w_0. In the simplest semi-empirical approximation we can just add to the expression for a in (3.3a) a term χw_0 with $\chi \approx 1$,

$$a = l\mu + \chi w_0, \qquad (5.1)$$

with corresponding changes in formulas (3.3), (3.4). l and μ are still given by (3.2). With high laser powers $l\mu \gg \chi w_0$ and the first term in (5.1) exceeds the second so that original expressions are obtained. For low laser powers $l\mu \ll \chi w_0$ and the width becomes practically independent of P and is determined by the second term in (5.1):

$$r(\theta_c) \approx \xi\chi w_0,$$

$$h(\theta_c) = (\zeta\xi\chi\eta)^{-1}\frac{P^2A^2}{w_0 K_S K_D \theta_c^2}e^{-2\mu}, \qquad (5.2)$$

$$v_s(\theta_c) = \gamma\frac{a}{h}W(T_c)$$

$$= \gamma\zeta\xi\eta\chi^2\frac{w_0^2 K_S K_D \theta_c^2}{P^2A^2}e^{2\mu}W(T_0 + \theta_c).$$

Thus, the width of the stripe is independent of power while its height is proportional to P^2.

In the absence of a threshold but a high activation energy, $\mu \ll 1$ and $\theta_e \approx \theta_c \approx T_c$ (see (4.4)). Then, approximately $r(v_s) \approx$ const, $h(v_s)$ a P^2[const – $\ln(v_s)$]^2.

5.2. Temperature dependence of heat conductivities

Up to now we have assumed that the heat conductivities of substrate and deposit are constants. Arbitrary temperature dependences of heat conductivities

can be incorporated into the model via the Kirchhoff transform [7]. Then, instead of (3.1) we obtain

$$l^2\frac{\partial^2\theta_D}{\partial x^2} - \theta_S(\theta_D) + \frac{PA}{\eta K_S}\delta(x) = 0. \qquad (5.3)$$

Here K_S, K_D, should be taken at $T = T_0$, and $\theta_S(\theta_D)$ is given by the relation $T(\theta_D) = T(\theta_S)$ which holds for the interface between the deposit and the substrate. Eq. (5.3) is easily solved together with the boundary conditions in (3.1) using the conservation law:

$$\frac{l^2}{2}\left(\frac{\partial\theta_D}{\partial x}\right)^2 - g(\theta_D) = \text{const},$$

with

$$g(\theta_D) = \int_0^{\theta_D}\theta_S(\theta)\,d\theta. \qquad (5.4)$$

Using (5.4), after some calculations we obtain instead of (3.2ab):

$$\mu(\theta_c) = \frac{a}{l} = \int_{\theta_e}^{\theta_c}\frac{d\theta}{\{2[g(\theta) - g(\theta_e)]\}^{1/2}}, \qquad (5.5a)$$

$$l = \frac{PA}{\eta K_S}\left\{[2g(\theta_c)]^{1/2} + [2g(\theta_c) - 2g(\theta_e)]^{1/2}\right\}^{-1}, \qquad (5.5b)$$

Then, we substitute I and μ in (3.3) and (3.4).

If the threshold is important, $\theta_e = \theta_{th} = \text{const}$, and from (5.5a) we find that μ increases with θ_c. Thus, nonlinearities in $K(T)$ do not cause qualitative changes in the dependences $r(v_s)$ and $h(v_s)$. Without any threshold, θ_e is not constant. For a high T_a, the value of T_e is close to T_c (see (4.3a)) and this is the case also for θ_e and θ_c. Then, we can use a Taylor expansion for θ_e, $\mu(\theta_c)$, $I(\theta_c)$, etc. Corresponding formulas show, that $\mu(\theta_c)$ can start to decrease with T_c. Consequently, the width or height of stripes can increase with v_s if the exponent m in the corresponding parametric dependence r, h $a\ T_c^m$ is positive. For the power dependences of the heat conductivities of the deposit and the substrate, $K_{D,S}$ $a\ T^{n_{D,S}}$, we obtained the following picture in the (n_D, n_S) plane (Fig. 4).

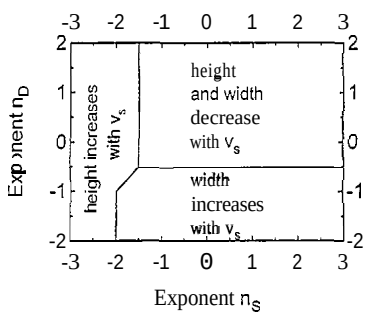

Fig. 4. The dependence of h and r on v_s for temperature-dependent heat conductivities $K_{D,S}(T)\ a\ T^{n_{D,S}}$. n_D and n_s refer to the deposit and the substrate, respectively.

6. Temperature dependence of absorptivity, oscillations

The temperature dependence of the absorptivity $\mathbf{A} = A(T)$ can be due to different reasons: changes in morphology, surface chemistry, optical properties, etc. Here, we assume that $A(T)$ function is known and $dA/dT > 0$. We employ (5.1) for a (w_0 is comparable with r) and (4.1) for θ_e (deposition with threshold). This corresponds to the case of W deposition on quartz [8].

When the temperature increases, the input of energy into the system increases due to the increase in absorptivity which in turn increases the temperature. Then, due to the extensive growth, the cross section of the stripe also increases and the heat losses due to conduction along the stripe exceed the input of energy, so that the temperature drops again.

The state of the 'chemical reactor' mentioned in Section 3.3 is characterised by the temperature T_c and the height h. The width of the stripe changes fast in comparison to h and is related to T_c via (3.3a). If oscillations occur, h and T_c are not constant but change with time. At each moment we can estimate T_c using stationary formulas for the uniform stripe whose cross section now depends on time. This implies, that the spatial period of oscillations is' relatively long. The evolution of our 'reactor' can be described by two ordinary differential equations for T_c and h where T_c should be considered as 'fast' variable, i.e. it practically instantaneously relaxes to its zero isocline $h = h(T_c)$ which determines the equilibrium value of T_c for the current value of h. The time of this relaxation is about l^2/D_T. Then,

the slow variable h changes according to its own evolutionary equation while T_c is related to h via the equation for T_c-zero isocline. The zero isoclines for T_c and h are given by (3.3b) and (3.4) respectively, with a taken from (5.1):

$$h(\theta_c) = \frac{\eta}{\zeta\xi K^*} \frac{l^2}{(l\mu + \chi w_0)}, \tag{6.1a}$$

$$h(\theta_c) = \gamma \frac{l\mu + \chi w_0}{v_s} W(\theta_c), \tag{6.1b}$$

where l depends on P and $A(T)$. If A is constant, we obtain from (6.1a) the dashed curve III in Fig. 5. Then, the system reaches the stable equilibrium position 4 which is given by the intersection of curve III with the zero isocline for h (6.1b), curve I.

For $A = A(T)$, the 6,-zero isocline is given by curve II. Here, the dependence

$$A(T) = A_0 + A_1\{\exp[(T_A - T)/\Delta T] + 1\}^{-1} \tag{6.2}$$

has been employed. AT characterises the width of the temperature interval near T_A where a drastic increase in absorption takes place. Now the system first relaxes to the 6,-zero isocline (curve II), but then it cannot reach the equilibrium point 1, which is unstable, but jumps from one branch of curve II to another at points 2 and 3 which are minimum and maximum of the curve II. Thus, the system ends up in a limit cycle, demonstrating an oscillatory behaviour.

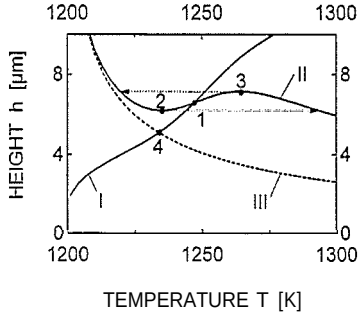

Fig. 5. Phase portrait of deposition process in the $(T_c, 11)$-plane (see text) calculated from (6.1a, b), (4.1) and (6.2) with $\chi = 1.0$, $A, = 0.45$, $A, = 0.45$, $T_a = 1250$ K, $AT = 10$ K, $v_s = 1.5\times10^{-3}$ cm/s, $w_0 = 7.5\times10^{-4}$ cm. Other parameters are the same as for Fig. 2. For dashed line $A, = 0$. I: h-zero isocline (6.1b), II, III: T_c-zero isocline (6.1a). 1, 4: stationary points. Arrows indicate limit cycle for $A = A(T)$.

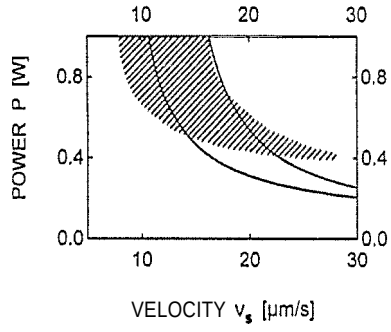

Fig. 6. Region of oscillations in the (P, v_s)-plane as calculated from (6.3), with (6.1), (4.1) and (6.2). Paramctcrs arc the same as in Fig. 5. Shaded area indicates region where oscillations have been observed experimentally for W dcpasition from WCl_6 [8].

Oscillations cart occur if *the only* equilibrium point 1 is situated between points 2 and 3. These extrema exist only if $A(T)$ is steep enough to ensure, that energy input is more sensitive to temperature changes then the heat losses (positive feedback). An oscillatory type of the intersection between the isoclines will take place, if curve I is below curve II at $\theta_c = \theta_2$, and above it at $\theta_c = \theta_3$, i.e. (see (6.1)) for:

$$\frac{W(\theta_c)}{v_s} < \frac{\eta}{\gamma\zeta\xi K^*} \frac{l^2}{(l\mu + \chi w_0)^2}\bigg|_{\theta_c = \theta_2},$$

$$\frac{W(\theta_c)}{v_s} > \frac{\eta}{\gamma\zeta\xi K^*} \frac{l^2}{(l\mu + \chi w_0)^2}\bigg|_{\theta_c = \theta_3}. \tag{6.3}$$

The region in the $(P, 1;)$-plane where oscillations occur (given by (6.3)) for the case of W deposited on quartz is depicted on Fig. 6. For low laser powers $l\mu \ll \chi w_0$, and we can derive from (6.3) that the boundaries of this region are $C_1 v_s^{-1/2} < P < C_2 v_s^{-1/2}$. With increasing scanning velocity this region becomes very thin and in experiments can even disappear. With high laser powers the region where oscillations occur is between two lines, parallel to the P-axis in the $(v_s$, P)-plane. Fig. 6 shows semi-quantitative agreement with experimental results.

7. Temperature gradient in z-direction – discontinuous deposition

Up to now we have assumed that the temperature in z-direction is uniform. This is a good approxima-

tion for thin stripes. In reality, however, the temperature at the surface of the deposit is somewhat higher than at the interface to the substrate. This difference becomes more pronounced with increasing thickness of the stripe. The effect can be estimated by employing a Taylor expansion:

$$T_D|_{z=h} \approx T_D|_{z=0} + h\left.\frac{\partial T_D}{\partial z}\right|_{z=0}. \tag{7.1}$$

The derivative can be determined from the continuity of the heat flux at $z=0$, and we used an estimation $\partial T_s/\partial z|_{z=0} \approx \theta_s/r$. This yields for θ_c:

$$\theta_c|_{z=h} = \left(1 + \frac{\delta}{K^*}\frac{h}{r}\right)\theta_c|_{z=0}. \tag{7.2}$$

Here, the coefficient $6 \approx 1$ accounts for uncertainties in the approximations. For $h/r = 1$, $K^* = 10$, $\theta_c \approx 2 \times 10^3$ K, the difference between the temperature at $z=h$ and at $z=0$ can reach hundreds of kelvin, which is crucial for the deposition with high activation energies.

This can lead to the following phenomena: Let us consider two points at the surface of the stripe – near the edge $x=a$, and near $x=0$. With decreasing v_s both $T_c(z=0)$ and T_e decrease, because of the increasing cross section of the stripe. From the other point of view, the stripe becomes thicker, so that the temperature at the surface of the deposit near $x=0$ increases, due to the second term in (7.2). The ratio of growth rates at the surface of the deposit at points $x=0$ and $x=a$ is determined by the difference in corresponding temperatures. But the temperature T_e at $x=a$ does not contain the increasing term due to the temperature gradient in the z-direction. With decreasing scanning velocities the ratio h/r increases, thus increasing the ratio of growth rates. Growth is perpendicular to the surface of the deposit and with $h/r \approx 1$ the vector of growth has considerable components in the x-direction. Thus, at low scanning velocities growth near $x=a$ cannot keep up with growth near $x=0$. Therefore, there exists a minimum scanning velocity below which continuous deposition of a stripe with finite slope near its edge becomes impossible. As a consequence, the stripe will tend to turn over like the front of a nonlinear wave. This was observed during deposition of Si [9] and C [10] on glass. Let us incorporate this physical picture into our model. The position of the edge of the stripe is determined by (4.2), but T_e and T_c have a different meaning now. T_e denotes the temperature at the edge of the stripe, i.e. at $x=a$, $z=0$. Therefore, T_e is exactly T_e which enters the boundary conditions of the heat equation and formulas (3.2), (3.3). T_c on the right side of (4.2) is now the temperature at the surface of the deposit and should be taken from (7.2). Now we can rewrite the relationship (4.3) between θ_e and θ_c in terms of θ_c, θ_e, and T_c at $z=0$, which enter (3.1) and the subsequent formulas. With $\epsilon = \delta h/K^* r$ we obtain for small ϵ and T_c/T_a:

$$\begin{aligned}\theta_e(\theta_c) &\approx \theta_c\left[1 + \epsilon\left(1 - \frac{2\beta T_c}{T_a}\right) - \frac{\beta T_c^2}{\theta_c T_a} + \frac{T_c}{\theta_c}\left(\frac{\beta T_c}{T_a}\right)^2\right] \\ &\approx \theta_c\left(1 + \epsilon - \frac{\beta T_c}{T_a}\right).\end{aligned} \tag{7.3}$$

The term with ϵ is due to the temperature difference in the z-direction. Clearly, $\epsilon \ll 1$, because $K^* \gg 1$.

Let us find μ. ϵ is a function of μ and we write instead of (3.2a):

$$\frac{\theta_e}{\theta_c} = \cosh^{-1}\mu \tag{7.4a}$$

$$= 1 + \frac{\epsilon_0}{\mu^2} - \beta_0, \tag{7.4b}$$

with

$$\epsilon_0 = \frac{\delta\eta}{\xi^2\zeta K^{*2}}\left(1 - \frac{2\beta T_c}{T_a}\right) \approx \frac{\delta\eta}{\xi^2\zeta K^{*2}} \ll 1,$$

$$\beta_0 = \frac{\beta T_c^2}{\theta_c T_a} - \frac{T_c}{\theta_c}\left(\frac{\beta T_c}{T_a}\right)^2 \approx \frac{\beta T_c}{T_a} \ll 1.$$

As will be confirmed later, $\mu \ll 1$, and we can expand cosh μ in a Taylor series. This gives a biquadratic equation for $m = \mu^2$ with the solutions:

$$\mu = m^{1/2} = \left[\beta_0 \pm \left(\beta_0^2 - 2\epsilon_0\right)^{1/2}\right]^{1/2}. \tag{7.5}$$

In (7.5) only the '+' sign is physical, because it gives the right answer for $\epsilon = \epsilon_0 = 0$. As long as a solution exists, $\mu \approx \beta_0^{1/2} \ll 1$. This justifies the

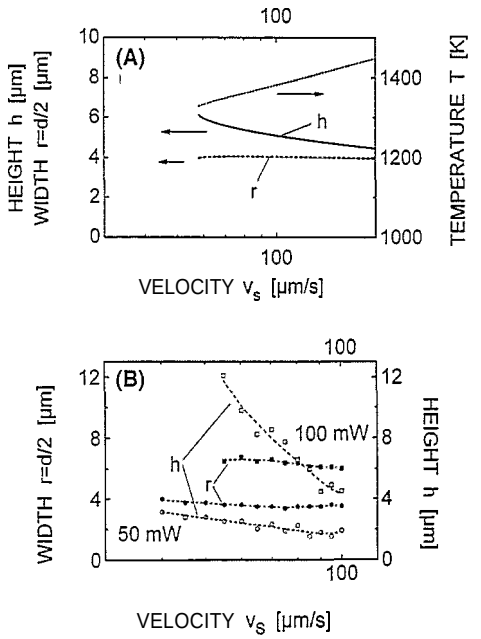

Fig. 7. **(A)** The discontinuous deposition at low scanning velocities due to finite thickness of the stripe as calculated from (3.2b)–(3.3), (7.6), (4.3) and μ given by (7.5). $\delta = 0.3$, other parameters are as in Fig. 3. (B) The same picture determined experimentally for two different laser powers for the deposition of Si from SiH_4 on glass [9].

Taylor expansion (7.4). With the knowledge of μ we can draw the parametric dependences $h(v_s)$, $r(v_s)$ using θ_c as a parameter in the usual way. When h/r is about unity, growth takes place in the direction perpendicular to the surface. For that reason, the term $\gamma a/h$ in (3.4) should be replaced by $(\gamma a/h)(1 + (h/\gamma a)^2)^{1/2}$, giving instead of (3.4):

$$v_s \approx \frac{\gamma}{\xi}\frac{r}{h}\left[1 + \left(\frac{\xi h}{\gamma r}\right)^2\right]^{1/2} W(T_c + \epsilon\theta_c). \qquad (7.6)$$

Note, that the rate function is taken at the temperature at *the* surface of the deposit. The model calculations presented at Fig. 7A simulate the experimental data for $\mathbf{P} = 100$ mW in Fig. 7B. Real solutions exist as long as $\beta_0^2 - 2\epsilon_0 > 0$. That gives (see (7.4))

$$\frac{\beta T_c}{T_a} > \left(\frac{2\delta\eta}{\zeta\xi^2}\right)^{1/2} K^{*-1}. \qquad (7.7)$$

Thus, the solutions disappear at low T_c, i.e. at low v_s. At this critical point

$$\mu_{cr} = (\beta_0)^{1/2} = (2\epsilon_0)^{1/4} \approx \left(\frac{2\delta\eta}{\xi^2\zeta}\right)^{1/4} K^{*-1/2} \ll 1, \qquad (7.8a)$$

$$\epsilon_{cr} = \frac{\epsilon_0}{\mu_{cr}^2} = \left(\frac{\epsilon_0}{2}\right)^{1/2} \approx \left(\frac{\delta\eta}{2\xi^2\zeta}\right)^{1/2} K^{*-1} \ll 1, \qquad (7.8b)$$

$$\frac{h_{cr}}{r_{cr}} = \frac{K^*}{6}\epsilon_{cr} = \frac{K^*}{\delta}\left(\frac{\epsilon_0}{2}\right)^{1/2} \approx \left(\frac{\eta}{2\delta\xi^2\zeta}\right)^{1/2} \sim 1. \qquad (7.8c)$$

The temperature T_{ccr} can be estimated in a crude way from (7.7). It depends on K^* and T_a only. With high laser powers v_{scr} depends on the properties of the substrate, T_a, and the pressure of the precursor gas only, and it is given by (7.6) where one should use critical values.

From (7.8b) we find $\epsilon_{cr} \ll 1$, which is also true for sub critical values of E, because then $\mu > \mu_{cr}$. This confirms the Taylor expansion in the z-direction. There is no singularity when the solution disappears: all quantities are finite. The critical ratio of the height/width turns out to be dependent only on geometrical factors and it is about unity. Thus, there is no hope to produce 'wall-type' structures. The height of the stripe can become of the order of its width, or a continuous deposition breaks off.

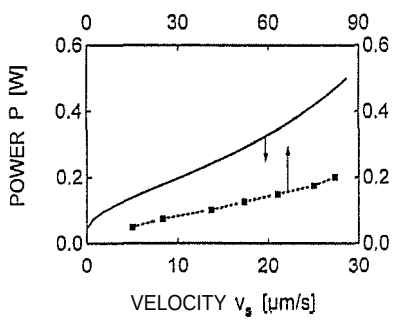

Fig. 8. The dependence of the critical velocity on laser power $v_{scr}(P)$ as calculated from (7.10) (T_{ccr} and μ_{cr}), (3.3) with a from (5.1) for r_{cr} and h_{cr}, and (7.6) for v_{scr}. $\delta = 0.3$, $\chi = 0.3$, $w_0 = 3\times10^{-4}$ cm. Other parameters are the same as for Figs. 3 and 7. Note the difference in scale for theoretical (full line) and experimental (Si from SiH_4, dashed line) curves.

For finite laser focus we have to employ the formulas given in Section 5.1. Thus we can repeat the derivation of (7.4) with the same $\epsilon = \delta h / K^* r$. However, ϵ cannot be replaced by ϵ_0/μ^2, because the expressions for h and r are now different. Instead of (7.4) we obtain:

$$\frac{\theta_e}{\theta_c} = \cosh^{-1}\mu = 1 + \frac{\epsilon_0}{[\mu + (\chi w_0/l)]^2} - \beta_0 \tag{7.9}$$

which can be approximated by:

$$\mu^2(\mu+\omega)^2 - 2\beta_0(\mu+\omega)^2 + 2\epsilon_0 = 0,$$

with

$$\omega = \frac{\chi w_0}{l} \approx \chi\eta\frac{w_0 K_S \theta_e}{PA}, \tag{7.10}$$

This permits the determination of μ. We are interested in the influence of a finite w_0 on the critical parameters. The biggest root of (7.10) disappears at $\mu_{cr} = [(\omega^2 + 16\beta_0)^{1/2} - \omega]/4$. Solving (7.10) together with P,, we find $T_{c\,cr}$ and then determine μ, l, r, h, v_s at the critical point. Note that β_0, ϵ_0, and ω depend on T_c and P. The plot $P_{cr}(v_s)$, obtained by this procedure is presented in Fig. 8. P_{cr} increases with v,. This increase is due to the finite size of laser focus w_0. Otherwise v_{cr} does not depend on P. This is in qualitative agreement with the experiments on Si deposition from SiH_4. Note, however, the difference in velocity scales.

8. Conclusions

Many phenomena observed in laser direct writing can be explained on the basis of a one-dimensional approach. Among them are typical dependences of the height and width of stripes on scanning velocity and laser power, oscillations, and discontinuous deposition at low scanning velocities.

Acknowledgements

We wish to thank the 'Jubilaumsfonds der österreichischen Nationalbank' for financial support and Professor B.S. Luk'yanchuk and Dr. N.A. Kirichenko for useful discussions and critical comments.

References

[1] D. Bauerle, Chemical Processing with Lasers, Springer Ser. Mater. Sci. Vol. 1 (Springer, Berlin, 1986).
[2] N. Arnold, R. Kullmer and D. Bauerle, Microelectron. Eng. 20 (1993) 31.
[3] P.E. Price, Jr. and K.F. Jensen, Chem. Eng. Sci. 44 (1989) 1879.
[4] R. Kullmer, P. Kargl and D. Bauerle, Thin Solid Films 218 (1992) 122;
Z. Toth, P. Kargl, C. Grivas, K. Piglmayer and D. Bauerle, Appl. Phys. B 54 (1992) 189.
[5] G.Q. Zhang and D. Bäuerle, in: Proc. ICMPC'88, Shanghai (1988).
[6] W. Kräuter, D. Bauerle and F. Fimberger, Appl. Phys. A 31 (1983) 13.
[7] M. Lax, Appl. Phys. Lett. 33 (1978) 786.
[8] P. Kargl, R. Kullmer and D. Bauerle, Appl. Phys. A 57 (1993) 175.
[9] P. Kargl, R. Kullmer and D. Bauerle, Appl. Phys. A 57 (1993) 577.
[10] P. Kargl, N. Arnold and D. Bauerle, to be published.